Astro2020 Science White Paper

Robustly Mapping the Distribution of Star Formation in High-z Galaxies

Thematic Areas: ☐ Planetary Systems ☐ Star and Planet Formation
☐ Formation and Evolution of Compact Objects ☐ Cosmology and Fundamental Physics
☐ Stars and Stellar Evolution ☐ Resolved Stellar Populations and their Environments
☑ Galaxy Evolution ☐ Multi-Messenger Astronomy and Astrophysics

Principal Author:
Name: Eric J. Murphy
Institution: National Radio Astronomy Observatory
Email: emurphy@nrao.edu
Phone: 434-296-0373

Co-authors: Chris Carilli (NRAO), **Lee Armus** (Caltech/IPAC), **Amy J. Barger** (U. Wisconsin-Madison), **Alberto Bolatto** (U. Maryland), **Denis Burgarella** (Aix-Marseille University), **Peter Capak** (Caltech/IPAC), **Caitlin Casey** (UT-Austin), **Ranga-Ram Chary** (Caltech/IPAC), **Asantha Cooray** (UC Irvine), **James J. Condon** (NRAO), **Tanio Diaz Santos** (Universidad Diego Portales), **Mark Dickinson**(NOAO), **Carl Ferkinhoff** (Winona State University), **Allison Matthews** (UVa), **Desika Narayanan** (U. Florida), **Kotaro Kohno** (Tokyo University), **Alex Pope** (UMass Amherst), **Dominik Riechers** (Cornell), **J.D. Smith** (Toledo), **Mark T. Sargent** (Sussex), **Douglas Scott** (UBC), **Fabian Walter** (MPIA, NRAO)

Abstract: The bulk of the present-day stellar mass was formed in galaxies when the universe was less than half its current age (i.e., $1 \lesssim z \lesssim 3$). While this likely marks the most critical time period for galaxy evolution, we currently do not have a clear picture of the radial extent and distribution of star formation within the disks of galaxies during this epoch. The lack of a reliable, dust-unbiased measurement for such a fundamental parameter as the size of a galaxy's star-forming disk, let alone how star formation activity is distributed within it, is extremely unsatisfactory, but also beyond the capabilities of current facilities. To make the next transformational step in our understanding of galaxy formation and evolution requires the ability to simultaneously study the relative distributions of the atomic and molecular gas, stellar mass, and current (i.e., $\lesssim$ few Myr) star formation activity on sub-kpc scales (i.e., $\lesssim 0\farcs1$ resolution at $z \gtrsim 1$) unbiased by dust for large populations of typical galaxies in the early universe.

Introduction

In standard cosmological models, baryonic material flows into the gravitational potential wells of dark matter halos as they coalesce out of an otherwise expanding universe. This gas cools, condenses, and eventually fuels star formation in early galaxies. The physical processes suggested for triggering, modulating, and even suppressing star formation are numerous and still poorly understood. On very small scales, we have observed that the instantaneously available local fuel supply must play a crucial role in star formation (e.g., Kennicutt 1998, Bigiel 2008; Leroy et al. 2008). Furthermore, when observed on the largest scales, the galaxy clustering environment also clearly plays an important role in the rate of star formation (e.g. Dressler et al., 1997; Butcher & Oemler, 1978, 1984; Desai et al., 2007). To piece together a fully consistent, predictable theory of star formation requires tracing each of these processes on the full range of scales that they operate for a large, heterogeneous set of physical conditions. While nearby galaxies and our own Milky Way provide the best means to study the small scale physics directly, it is critical that we relate such investigations to the intensity and distribution of star formation *within* large samples of "typical" galaxies when the majority of the present day stellar mass was produced (i.e., $1 \lesssim z \lesssim 3$; Madau & Dickinson, 2014 and references therein). Our current inability to bridge the gap between star formation studied on sub-kpc scales within nearby galaxies to globally integrated measurements of large populations of galaxies at high-redshifts remains a major impediment to progress in our understanding of galaxy formation and evolution.

What is the size distribution of star-forming galaxy disks at $z \gtrsim 1$ and how is star formation activity distributed within them? How does this distribution compare to that of the stellar mass and molecular gas at these epochs? Is star formation clumpy and distributed as inferred from rest-frame UV observations of high-z galaxies, or is this purely an artifact of spatially varying dust obscuration as currently indicated by observations of cold dust in such systems? Is star formation more centrally concentrated?

Observations in the rest-frame UV, optical (Hα), sub-mm (cold dust), low-frequency radio (synchrotron), and high-frequency radio (free-free) all suggest different typical sizes of $1 \lesssim z \lesssim 3$ star-forming disks in the few tenths of an arcsecond ($\lesssim 1-5$ kpc) range (e.g., Nelson et al. 2016; Ikarashi et al. 2015; Simpson et al. 2015; Murphy et al. 2017; Bondi et al. 2018; Cotton et al. 2018). Furthermore, nearly all such studies have been carried out for the different populations of galaxies. The fact that we do not have a reliable measurement for such a fundamental parameter as size, let alone the distribution of star formation, when galaxies were building the bulk of their stellar mass is astonishing, but also beyond the capabilities of extant facilities. Sub-arcsecond imaging of the gas, stellar mass, and current (i.e., $\lesssim$ few Myr) star formation activity unbiased by dust for large populations of typical galaxies in the early universe is a requisite for significant progress in the studies of galaxy formation and evolution.

The Energetic Processes Powering Radio Continuum Emission

Radio continuum emission from galaxies covering $\sim 1.2-116$ GHz is powered by an eclectic mix of physical emission processes, each providing completely independent information on the star formation and interstellar medium (ISM) properties of galaxies (see Figure 1). As such, radio continuum observations provide unique windows into the ISM and the process of star formation in galaxies. These processes include:

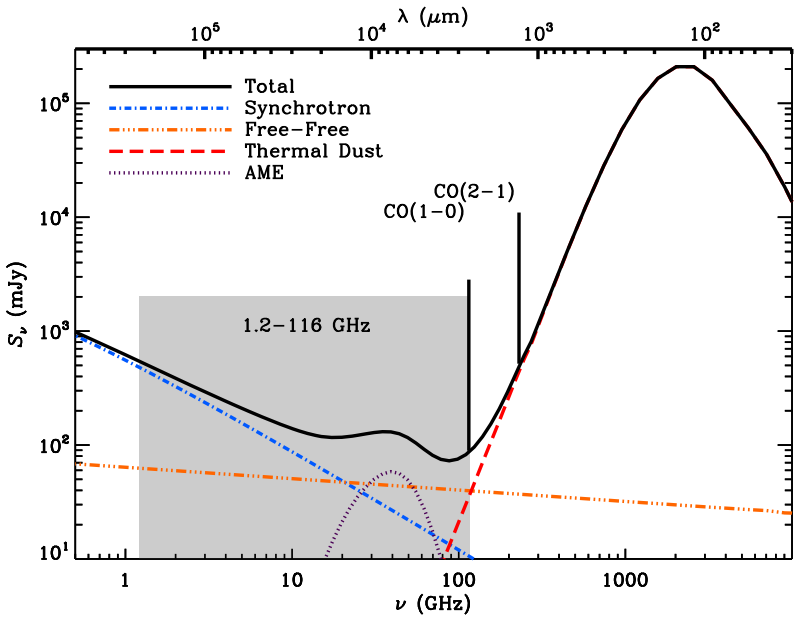

Figure 1: A model spectrum illustrating the various emission processes (non-thermal synchrotron, free-free, AME, and thermal dust) that contribute to the observed radio frequency range to be covered by the ngVLA. The proposed ngVLA frequency range ($1.2 - 116$ GHz) is highlighted, indicating that the strength of free-free emission relative to the other components increases with redshifts, indicating that such radio observations provide highly robust measures of massive star formation in galaxies. The $J = 1 \rightarrow 1$ and $J = 2 \rightarrow 1$ lines of CO are shown, for which some combination will be detectable at $1 \lesssim z \lesssim 3$. While a contribution form AME is illustrated in the figure, current observations of galaxies on kpc scales do not currently indicate a strong presence of AME.

- **non-thermal synchrotron emission** powered by cosmic-ray (CR) electrons/positrons accelerated by supernova remnants in a galaxy's magnetized ISM;
- **free-free emission** from the ionized gas in young massive star-forming (HII) regions;
- **anomalous microwave emission** (AME), which is a dominant, but completely unconstrained, foreground in cosmic microwave background (CMB) experiments;
- **cold, thermal dust emission** that accounts for most of the dust and total mass content of the ISM in galaxies.

Each of these emission mechanisms are directly related to the various phases of the ISM and provide a comprehensive picture of how galaxies convert their gas into stars. However, each component is also of low surface brightness in the (rest-frame) $\sim 30 - 120$ GHz frequency range, and therefore difficult to map in a spatially resolved manner at $\sim$kpc scales in high-z galaxies using extant facilities.

Globally, free-free emission begins to dominate the total radio emission in normal star-forming galaxies at $\gtrsim$30 GHz (e.g., Condon et al. 1992), with fractional contributions as high as 80% measured in nearby starbursts (i.e., M 82, NGC 253, and NGC 4945; Peel et al. 2011). Moreover, free-free emission is likely to become even more dominant at higher redshifts, due to increased energy losses of the synchrotron emitting relativistic electron population through inverse Compton (IC) scattering off of the photons in the strengthening CMB. Such energy losses are linearly proportional to the energy density of the CMB, which itself increases as $\sim (1+z)^4$ (e.g., Carilli 2001). Consequently, non-thermal emission from galaxies should become severely suppressed

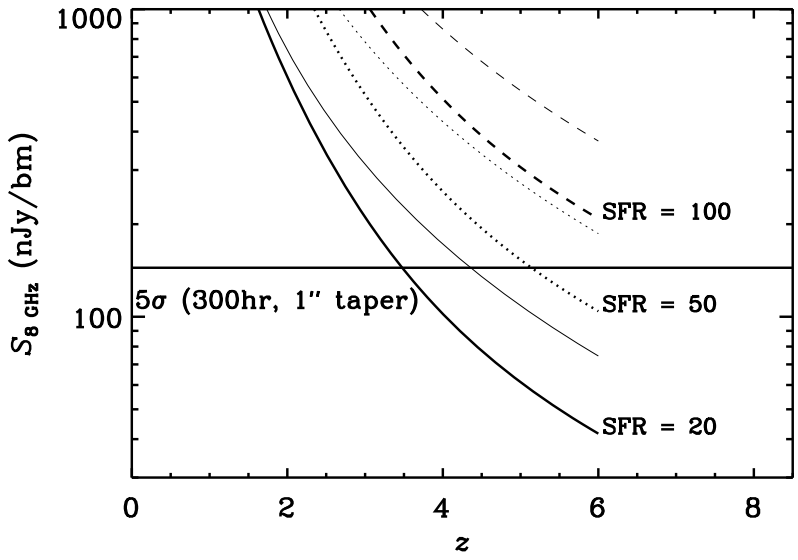

Figure 2: Telescope sensitivity in nJy bm^{-1} at 8 GHz plotted against redshift indicating the expected brightness of a 4 kpc disk galaxy forming stars at a rate of 20, 50, and 100 $M_\odot\,\mathrm{yr}^{-1}$ with a magnetic field strength of 35 μG (Murphy 2009). The heavy-weighted lines include estimates for synchrotron dimming due to IC scattering of CR electrons/positrons in galaxies due to the increasing CMB energy density with redshift, while the corresponding lighter-weighted lines indicate the expected brightnesses in the absence of any synchrotron dimming due to CMB effects. The horizontal line shows the sensitivity of a future large area array, such as the next-generation VLA. The ngVLA will have enough sensitivity to detect galaxies forming stars at a rates down to $\sim 50\,M_\odot\,\mathrm{yr}^{-1}$ into the Epoch of Reionization, while simultaneously resolving the structure of star-forming disks throughout "cosmic noon" (i.e., $1 \lesssim z \lesssim 3$), in observations of tens to 100 hours. Using the existing VLA would require $\gtrsim$10,000 hr!

with increasing redshift, making this frequency range ideal for accurate estimates of star formation activity at high z unbiased by dust (Condon 1992; Murphy 2009).

This effect is illustrated in Figure 2 where telescope sensitivity in nJy bm^{-1} at 8 GHz is plotted against redshift indicating the expected brightness of a 4 kpc disk galaxy forming stars at a rate of 20, 50, and 100 $M_\odot\,\mathrm{yr}^{-1}$. The heavy-weighted lines include estimates for synchrotron dimming due to IC scattering of CR electrons/positrons in galaxies due to the increasing CMB energy density with redshift, while the corresponding lighter-weighted lines indicate the expected brightnesses in the absence of any synchrotron dimming due to CMB effects. This expectation of synchrotron dimming is already hinted at given recent 10 GHz deep field observations for a sample of $z \gtrsim 1$ star-forming galaxies in GOODS-N, indicating that the rest-frame 20 GHz flux density appears to be dominated by free-free emission (i.e., $\gtrsim 50\%$; Murphy et al. 2017). It is worth noting that there is the possibility for a contribution from AME at these frequencies (e.g., Murphy et al. 2010, 2018a), which may arise from spinning dust grains (e.g., Draine & Lazarian 1998). However, current observations do not find a strong presence of AME both in globally-integrated and sub-kpc measurements of galaxies (see Astro2020 White Paper on AME by Murphy et al.).

What Could Be Possible in the 2030's?

What is ultimately required to make the next great leap in piecing together a self-consistent theory for star formation are robust, dust-unbiased maps of the current star formation activity for large,

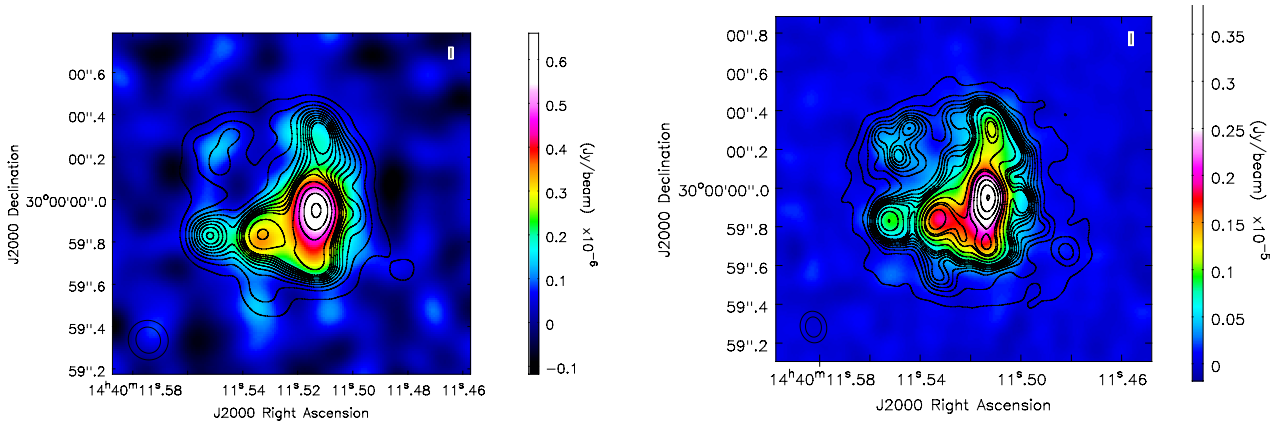

Figure 3: **Two simulated images of high-z galaxies mapped in their free-free emission, providing a robust (dust-unbiased) characterization of the extent and distribution of their star formation.** *Left:* A main sequence star forming galaxy of 50 $M_\odot$ year^{-1} at $z = 1$. The color scale shows a simulated observation with an rms noise of 32 nJy beam^{-1} for a synthesized beam FWHM = 0.″19 = 1.5 kpc. The black contours show the input model at 0.″12 resolution, with no noise added. *Right:* A massive starburst galaxy of 3000 $M_\odot$ year^{-1} at $z = 3$. The color scale shows the simulated observation with an rms noise of 49 nJy beam^{-1} for a synthesized beam FWHM = 0.″15 = 1.2 kpc. The black contours show the input model at 0.″09 resolution, with no noise added. Both simulations assume a deep ($\sim$ 100 hr) integration using what is being described as a next-generation VLA (Bolatto et al. 2017; Murphy 2018; Selina et al. 2018), as would occur in standard cosmological deep fields with the array, using the 16 GHz and 8 GHz bands (in the left and right panels, respectively) with a bandwidth of 8 GHz.

heterogenous samples of galaxies at $\lesssim$ kpc resolution at all redshifts. Consequently, a key capability needed in the coming decade is high resolution ($\lesssim$ 0.″1) imaging of galaxies during the epoch of peak galaxy assembly (i.e., $1 \lesssim z \lesssim 3$). It is possible that a next-generation of large spectroscopic surveys immune to the effects of dust could be used track the co-evolution of star formation and accretion energetics over cosmic time (e.g., see Astro2020 White Paper by Pope et al.), but investigating the detailed astrophysics of individual systems will require high-resolution follow-up that is also able to penetrate high columns of dust. A new window that will open with the advent of future large radio facilities will be the ability to image free-free emission from distant galaxies at rest frequencies of $\sim$ 30 GHz on these scales (Murphy et al. 2012, 2018b). To illustrate such capabilities, we present two test cases in Figure 3. First is a main-sequence star forming galaxy of 50 $M_\odot$ year^{-1} at $z = 1$ (left panel). Second is a massive starburst galaxy of 3000 $M_\odot$ year^{-1} at $z = 3$ (right panel).

As a template for the spatial distribution of the rest-frame 32 GHz emission, we adapt an observation of the Hα emission from NGC 5713 (Kennicutt et al. 2003), a star-forming disk galaxy at a distance of 21 Mpc. The Hα image suffers from both dust extinction and contamination from nearby [NII] line emission, so its relation to the free-free emission is only illustrative. We then adjust the observing frequency, spatial scale, and flux density to correspond to a 50 $M_\odot$ year^{-1} star-forming galaxy at $z = 1$, based on the relationships from Yun, Reddy & Condon (2001), and using a spectral index of -0.7 (adjusted for flattening in the frequency range in which free-free emission likely becomes prominent).

The simulations employ the latest configuration and parameters for the next generation Very Large Array main array, which is comprised of 214 $\times$ 18m antennas with baselines to a 1000 km (Selina et al. 2018). We assume a deep integration of 100 hrs, as would occur in standard cos-

mological deep fields with the array, using a bandwidth of 8 GHz. The result for a main-sequence star-forming galaxy at $z = 1$ observed at 16 GHz are shown in the left panel of Figure 3. The imaging uses *Briggs* weighting ($R = -0.5$) and a (*u,v*)-taper of $0\farcs17$, resulting in a synthesized beam FWHM = $0\farcs19$ = 1.5 kpc. The color scale shows the mock ngVLA observations with noise, at $0\farcs19$ resolution. The black contours show the input model at $0\farcs12$ resolution, with no noise added. The total flux density of the source at the observing frequency of 16 GHz is 3.1 μJy and the peak is $0.66\,\mu$Jy beam^{-1}. The rms noise is 32 nJy beam^{-1}, about a factor 1.6 higher than Natural weighting due to the (*u,v*)-weighting employed. The ngVLA would image emission across the disk at 1.5 kpc resolution, down to surface brightnesses of $\sim 0.13\,\mu$ Jy beam^{-1}, or star formation surface densities of $\sim 1\,M_\odot$ kpc^2 year^{-1}.

We perform a similar mock observation of a luminous starburst at $z = 3$, with a star formation rate of ~ 3000 M$_\odot$ year^{-1}, comparable to the most extreme starbursts in the early Universe (e.g., bright sub-mm and dusty quasar host galaxies). The result of an 8 GHz observation (32 GHz rest-frame) with a resolution of $0\farcs15$ (1.2 kpc) is shown in the right panel of Figure 3, with an rms noise of 49 nJy beam^{-1}. The total flux density is 23 μJy, and the peak surface brightness is 3.9 μJy beam^{-1}. The contours show the input model with no noise at $0\farcs09$ resolution, for reference. Structure is clearly traced on ~ 1.2 kpc scales, down to surface brightness of $\sim 0.2\,\mu$Jy beam^{-1}, or star formation rate surface densities of $\sim 20 M_\odot$ kpc^2 year^{-1}.

These simulations indicate that imaging the rest-frame ~ 32 GHz emission from high redshift galaxies at $\sim$ 1 kpc resolution is clearly plausible with future large radio arrays, both for main sequence galaxies at $z \sim 1$, and luminous starbursts at $z \sim 3$. It is worth stressing that that these mock observations are an order of magnitude deeper than what is possible with current facilities, even with extreme integrations. At rest-frame 32 GHz, the emission is likely dominated by thermal free-free emission (e.g., Murphy et al. 2017), thereby providing the most direct measurement of the ionizing photon flux of the galaxy, and hence star formation rate (modulo an IMF), without questions of obscuration or empirical conversion factors.

Similar observations in the radio will deliver molecular gas distributions and dynamics, providing complementary information on star formation and AGN fueling (See the Astro2020 White Paper by C. Carilli). Such observations would definitively measure the physical extent of star formation in typical $z \gtrsim 1$ galaxy disks, which currently remains unknown and highly debated (see Introduction). Furthermore, the free-free emission maps discussed here should prove fundamental for metallicity determinations of galaxies at all redshifts given that they provide a dust-unbiased means to normalize metal lines to the hydrogen abundance. For instance, combining observations of the collisionally excited pair of far-infrared [OIII] fine-structure lines (e.g., from *Origins*) with corresponding free-free maps may prove to be among the most unbiased means to measure absolute abundances in galaxies (See Astro2020 White Paper by J.D. Smith et al.). Coupling free-free continuum maps with large, spectroscopic maps of near-/mid-infrared H-recombination line maps (e.g., from *JWST*), which in the absence of significant dust extinction will deliver an equally robust estimate for the current star formation activity, can be used to estimate electron temperatures of the ionized gas. This is a critical ingredient when trying to assess metallicities from more common gas metal-abundance measures that (unlike far-infrared fine structure lines) suffer from temperature uncertainty. Such observations are clearly required to make the next transformational step for studies of star formation and chemical enrichment in the early universe.

References • Butcher, H., & Oemler, Jr., A. 1978, ApJ, 219, 18; • Butcher, H., & Oemler, Jr., A.1984, ApJ, 285, 426; • Bigiel, F., et al. 2008, AJ, 136, 2846; • Bolatto, A., et al. 2017, arXiv:1711.09960.; • Bondi, M., et al. 2018, A&A, 618, L8; • Carilli, C.L. 2001, in *Starburst Galaxies Near and Far*, eds. Taconni & Lutz, Springer Verlag, P. 309 • Condon, J. J. 1992, ARA&A, 30, 575; • Cotton, W. D., et al. 2018, ApJ, 856, 67; • Desai, V., et al. ApJ, 660, 1151; • Draine B. T., & Lazarian A. 1998, ApJ, 508, 157; • Dressler, A. et al. 1997, ApJ, 490, 577; • Hensley B. S., et al. 2015, MNRAS, 449, 809; • Hopkins P. F., Quataert E., Murray N., 2011, MNRAS, 417, 950 • Hopkins P.F.,KeresD.,OnorbeJ.,Faucher-GiguereC.- A., Quataert E., Murray N., Bullock J. S., 2014, MNRAS, 445, 581 • Hopkins P. F., et al., 2018b, MNRAS, 480, 800 • Ikarashi, S., et al. 2015, ApJ, 810, 133; • Kennicutt, R. C., Jr. 1998, ApJ, 498, 541 • Kennicutt, R, C., Jr., et al. 2003, PASP, 115, 928; • Leroy, A. K., et al. 2008, AJ, 136, 2782 • Madau & Dickinson, 2014, ARA&R, 52, 415; • Murphy E. J., 2009, ApJ, 706, 482; • Murphy E. J., et al. 2010, ApJL, 709, 108; • Murphy, E. J., et al. 2017, ApJ, 839, 35; • Murphy E. J., et al. 2018a, ApJ, 862, 20; • Murphy E. J., et al. 2018b, ApJS, 234, 24; • Murphy E. J. 2018, ASPC, 517, 3; • Nelson, E. J., et al. 2016, ApJL, 817, L9; • Peel M., et al. 2011, MNRAS, 416, L99; • Selina, R. J., et al. 2018, Science with a Next Generation Very Large Array , 517, 1; • Simpson, J. M., et al. 2015, ApJ, 799, 81; • Yun, M. S., et al. 2001, ApJ, 554, 803